Treatment of Cells with the Angiogenic Inhibitor Fumagillin Results in Increased Stability of Eukaryotic Initiation Factor 2-Associated Glycoprotein, p67, and Reduced Phosphorylation of Extracellular Signal-Regulated Kinases†

Bansidhar Datta,* Avijit Majumdar, Rekha Datta, and Ramesh Balusu‡

Department of Chemistry, Kent State University, Kent, Ohio 44242

Received April 24, 2004; Revised Manuscript Received September 16, 2004

ABSTRACT: Fumagillin, an angiogenic inhibitor, binds to methionine aminopeptidase 2, which is the same as eukaryotic initiation factor 2-associated glycoprotein, p67. p67 protects eIF2α from phosphorylation by its kinases. To understand the importance of fumagillin binding to p67, we measured the level of p67 in mouse C2C12 myoblasts treated with fumagillin. We show that fumagillin increases the stability of p67 by decreasing its turnover rate. The increased levels of p67 result in inhibition of phosphorylation of extracellular signal-regulated kinases 1 and 2 (ERKs 1 and 2). p67 binds to these ERKs, and the 108−480 amino acid segment is sufficient for this binding. p67's affinity to ERKs 1 and 2 also increases in fumagillin-treated myoblasts while its affinity for eIF2α remains unchanged. A mutant at the conserved amino acid residue D251A increases the phosphorylation of ERKs 1 and 2 without affecting the binding to p67, thus indicating the importance of this residue in the regulation of the phosphorylation of these ERKs. These results suggest that fumagillin increases the stability of p67 and its affinity to ERKs 1 and 2 and causes the inhibition of the phosphorylation of ERKs 1 and 2.

Angiogenesis is the process of forming new blood vessels from existing ones by either sprouting or splitting from their vessels of origin. This process has been shown to be necessary for tumor growth and metastasis (*1*, *2*). Several angiogenic inhibitors have been reported and can be classified into two major groups. One group belongs to proteins, and the other group is a collection of small molecules isolated from fungi or bacteria. Almost all of the known angiogenic inhibitors inhibit proliferation of endothelial cells. Protein angiogenic inhibitors are found in a fragment of a large protein which itself lacks inhibitory activity (*1*−*4*). Classified among the most potent small molecule inhibitors of angiogenesis is the fumagillin family of natural products. Fumagillin inhibits the proliferation of endothelial cells by arresting these cells at the G_1 phase of the cell cycle (*5*−*9*). Other reports claim that this drug blocks endothelial cells at both the G_1/S and G_2/M phases of the cell cycle (*3*, *4*, *8*, *9*). Biochemical analyses have suggested that the cellular target for fumagillin is methionine aminopeptidase 2, which is the same as p67[1] (for a review see ref *10*). p67 is a cellular glycoprotein that is associated with eukaryotic initiation factor 2 (eIF2) and plays a key role in the regulation of protein synthesis initiation (*10*−*14*). When the α-subunit of eIF2 is phosphorylated by its kinases, cell growth is restricted due to the inhibition of the overall rate of protein synthesis (*15*, *16*). However, this phosphorylation is blocked by p67 (*11*−*14*, *17*−*21*).

The 480 amino acid residues of mouse, rat, and human p67 are encoded by a recombinant ∼1.4 kb cDNA segment (*10*, *22*−*25*). Two lysine-rich domains (I and II) separated by an acidic residue-rich domain are present at the N-terminus (1−165 amino acid segment) of p67. These unique domains are highly conserved among mammals (*10*, *11*) and are involved in the regulation of activity toward the protection of eIF2α phosphorylation. There are also downstream sequences with consensus at $^{251}D(X)_{10}{}^{262}D(X)_{68}{}^{331}H(X)_{32}{}^{364}E(X)_{94}{}^{459}E^{460}H$ (see ref *10* and references cited therein and ref *26*). The side chains of these conserved amino acid residues are involved in coordinating with the Co^{2+} ion. X-ray crystallographic studies have indicated that the anti-angiogenic drug fumagillin binds covalently at the H231 residue of p67, and the conserved Co^{2+}-binding domain regulates such binding (*27*−*29*). The physiological effects of fumagillin binding to p67 are not clear at present. In this study, we have explored the molecular mechanisms of cell growth inhibition of mammalian cells by fumagillin by using mouse C2C12 myoblasts as a model system. We show that treatment of C2C12 myoblasts with fumagillin leads to the stabilization of p67. We also show that p67 binds to ERKs 1 and 2 and inhibits their activity.

MATERIALS AND METHODS

All chemicals used in this study were obtained from Sigma Chemicals (St. Louis, MO), Merck (Darmstadt, Germany),

† National Institutes of Health Grant GM59190 to B.D. supports this work.

* Corresponding author. Phone: (330) 672-3304. Fax: (330) 672-3816. E-mail: bdatta@kent.edu.

‡ Current address: UF Shands Cancer Center, University of Florida, 1600 SW Archer Road, ARB, R4-273, P.O. Box 100232, Gainesville, FL-32610-0232.

[1] Abbreviations: p67, eukaryotic initiation factor 2-associated 67 kDa glycoprotein; eIF2α, α-subunit of eukaryotic initiation factor 2 (eIF2); eIF2α(P), phosphorylated form of eIF2α; EGFP, enhanced green fluorescent protein; ERKs, extracellular signal-regulated kinases 1 and 2; p-ERK1/2, phosphorylated form of ERK1 and ERK2; IPs, immunoprecipitates; IB, immunoblotting; GST, glutathione *S*-transferase; MBP, myelin basic protein; PCR, polymerase chain reaction.

10.1021/bi049172p CCC: $27.50
Published on Web 10/30/2004

ICN Biomedicals, Inc. (Aurora, OH), Fisher Chemicals (Fair Lawn, NJ), or GIBCO-BRL (Rockville, MD). All enzymes used in this study were purchased from New England Biolabs (Beverly, MA). Different molecular mass markers were purchased from Bio-Rad. [^{35}S]Methionine and [γ-^{32}P]ATP were purchased from Amersham Corp.

Subcloning, Antiserum, Fumagillin, Cells, and Other Reagents. The entire coding region of rat p67 cDNA was amplified using PCR using appropriate primers containing *Bgl*II and *Not*I restriction sites. The cDNA insert was subcloned at these two sites in the pCMV-Myc vector (BD Biosciences/Clontech) to obtain in-frame fusion of wild-type p67 with the Myc epitope. Similar PCR reactions were performed to obtain the N-terminal 1−107 and 108−480 amino acid segments of p67, which were subcloned at *Bgl*II/*Not*I restriction sites in the pCMV-Myc vector. These plasmids were named Myc-p67, Myc-107, and Myc-p16, respectively. Flag-ERK1 and Flag-ERK2 plasmids were a gift of Drs. Andrew Catling and Steve Eblen (*30*).

Purification of p67 from rabbit reticulocytes was reported previously (*17*). A 1119 nucleotide long fragment of rat p67 encoding the 108−480 amino acid residues was amplified using PCR and subcloned into pGEX-1 (Glutagene Inc.) at its *BamHI* and *Sma*I sites to generate an in-frame fusion with glutathione *S*-transferase (GST). During polymerase chain reaction, a special forward primer was used. This primer has an extra nucleotide sequence encoding the enterokinase cleavage/recognition site (DDDDKD). The GST fusion protein was purified; the GST portion of the fusion protein was removed by digesting with enterokinase; the truncated version (108−480 amino acid residues) of p67 was gel purified and eluted. This eluted protein was mixed with Freund's complete adjuvant and injected into 4 week old female Balb/c mice. Two weeks after the first injection, subsequent boosters were given every week. During boosters, Freund's incomplete adjuvant was mixed with the protein sample. After three successive boosters, a small blood sample was collected from the immunized mice by tail bleeding. The titer of the antiserum was tested either by ELISA or immunoblotting. Once the titer reached 1:1000, freshly grown 180TG sarcoma cells were injected into the peritoneal cavity of the immunized mice. Two weeks later, the ascites fluid was collected. Cells from the serum were removed by centrifugation, and the clear ascites fluid was stored at −80 °C in aliquots. Similar procedures were followed to generate polyclonal antibodies against purified rabbit p67.

Generation of EGFP fusions of wild-type p67 and the D251A mutant was reported previously (*11*, *12*). Cell culture media, fetal bovine serum, dialyzed fetal bovine serum, horse serum, and insulin were purchased from GIBCO/Invitrogen Life Science Technology. C2C12 (ATCC 1172-CRL) murine thigh muscle myoblasts were used. Lipofectamine was purchased from GIBCO/Invitrogen. SuperFect transfection reagent was purchased from Qiagen. Fumagillin (catalogue no. 6771) from *Aspergillus fumgatus* was purchased from Sigma Chemicals (St. Louis, MO). Mouse monoclonal antibodies specific to α-actin (Sc-8432), p-ERK1/2 (Sc-7383), and ERK2 (Sc-1647) were obtained from Santa Cruz Biotechnology (Santa Cruz, CA). Anti-FLAG M2 monoclonal antibody specific to Flag epitope was purchased from Sigma, and anti-Myc monoclonal antibody specific to Myc-epitope was obtained from Clontech in a kit containing the pCMV-Myc vector. Rabbit polyclonal antibodies specific to ERK1 (Sc-94) and goat polyclonal antibodies specific to eIF2α were also obtained from Santa Cruz Biotechnology. ERK1 polyclonal antibodies recognize both ERK1 and ERK2 on Western blots. Similarly, a monoclonal antibody specific to p-ERK1/2 recognizes the phosphorylated forms of both ERK1 and ERK2. A monoclonal antibody specific to EGFP was purchased from Clontech. Polyclonal antibodies specific to p53 were purchased from Oncogene Life Science Technology. Glutathione−agarose-bound GST-ERK1 and myelin basic protein were purchased from Upstate Biotechnology (Lake Placid, NY); kinase-active ERK2 was purchased from New England Biolabs (Beverly, MA). GST-ERK1 was eluted from the beads by adding a 20 mM reduced form of glutathione.

Cell Growth, Fumagillin Treatment, Radiolabeling Cells, Pulse−Chase Experiment, Generation of Stable Cell Lines, Cell Lysis, Western Blotting/Immunoblotting, Immunoprecipitation, and Fluorography. C2C12 myoblasts were grown in Dulbecco's modified Eagle's medium (DMEM) supplemented with 10% fetal bovine serum under 5% CO_2−95% air at 37 °C. Fumagillin was dissolved in DMSO, and if so indicated, C2C12 myoblasts at 60% confluence were treated with 12 μM fumagillin for 24 and 36 h. Cells were labeled with [^{35}S]methionine, and pulse−chase experiments were carried out following the procedures as described (*14*). C2C12 myoblasts were transfected with highly purified p-EGFP vector, pEGFP-p67, and pEGFP-D251A plasmids using Lipofectamine. The transfected cells were then selected against G418 following the procedures as described (*14*). A total of 150−200 selected colonies were pooled, and cells were grown in cell culture dishes in the presence of G418. Whole cell lysates were prepared, protein concentrations were measured by Bio-Rad assay, and appropriate protein samples were used for Western blotting and immunoprecipitation experiments following the procedures as described (*14*). For immunoprecipitation assays, we take antibodies either from commercial sources or from antisera and allow binding to protein A−agarose first, microfuge to remove unbound antibodies or serum proteins, and add cell extracts to the antibody-bound beads. The amounts of antibodies used for immunoprecipitations vary from 5 to 10 μg depending upon the antigen being immunoprecipitated. Secondary antibodies used for this study were HRP-conjugated anti-mouse IgG and anti-rabbit IgG. For fluorographic experiments, samples were analyzed on a SDS−PAGE; the gels were incubated in a solution of 1 M sodium salicylate for 1 h, followed by drying and exposure to X-ray films. If not indicated, each experiment was repeated at least three times with similar results.

Transient Transfection Assay. Confluent cultures of C2C12 cells (50−60%) were transfected with plasmids complexed with SuperFect following protocols described by the manufacturer (Qiagen). After transfection (42 h), cells were harvested and cell lysates were prepared. Total cell extracts of 200−300 μg were used for immunoprecipitation experiments, and 50 μg of total protein samples was used for immunoblots. Transfection experiments were carried out in duplicate, and the experiments were repeated two times with similar results.

Determination of IC_{50} of Fumagillin in Mouse C2C12 Myoblasts. C2C12 cells (4×10^3) were seeded on a 24-well

tissue culture plate in quadruplet. The cells were grown for 24 h before addition of various concentrations of fumagillin varying from 0, 1.0, 2.5, 10.0, 50, and 100 nM in 0.5 mL of cell culture medium. Cells were incubated at 37 °C in a CO_2 incubator for 3 days. Viable cells were assayed using 3-(4,5-dimethylthiazol-2-yl)-2,5-diphenyltetrazolium bromide (MTT; Sigma Chemicals, St. Louis, MO) following the protocols as described (*31*). From four different experiments, the average IC_{50} was calculated to be 2.6 nM. The same experiments were repeated once with similar results.

Reverse Transcription−Polymerase Chain Reaction (RT-PCR). C2C12 myoblasts untreated or treated with fumagillin were grown, cells were harvested, and total RNA samples were isolated following the procedures as described (*32*). Two micrograms of total RNA samples was used for reverse transcription reactions using the RETROscript first strand synthesis kit (catalogue no. 1710) from Ambion following the manufacturer's protocols. Equal volumes of the samples from the reverse transcription reactions were used for polymerase chain reactions. The reaction conditions for PCR are as follows: hot start for 1 min, denaturation at 95 °C for 1 min, annealing at 54 °C for 1 min, and elongation at 72 °C for 3 min. The total numbers of cycles were 33, 35, and 37. The DNA samples were resolved on a 1.5% agarose gel and stained with ethidium bromide. Each RT-PCR reaction was repeated at least three times with similar results.

Expression and Purification of Proteins from Baculovirus-Infected Sf21 Cells. To generate recombinant viruses for protein expression in insect cells (Sf21), the entire coding region and the 5′ flanking region of rat wild-type p67 were subcloned into the BacPak8 vector (Invitrogen). To generate the recombinant baculovirus for the truncated version of p67 (containing the 108−480 amino acid segment), the cDNA insert corresponding to the amino acid segment was amplified using PCR and subcloned into the BacPak8 vector. The reverse primers were designed in a fashion such that the expressed proteins would have both the enterokinase recognition site and the cleavage site (DDDDKD) followed by 6×His tag at the C-terminus of the fusion proteins. To generate recombinant baculoviruses for wild-type p67, we followed protocols as recommended by the manufacturer (Clontech). For protein purification, Sf21 cells were infected with recombinant BacPak8 virus encoding p67 as a His-tag fusion protein. The fusion proteins were purified through Ni-NTA−agarose beads, dialyzed in PSSIV containing 100 mM KCl, analyzed on SDS−PAGE, and stained with Coomassie blue to check the purity. The purified His-tagged protein was then identified with specific polyclonal antibodies on a Western blot.

Stripping Off Antibodies from Western Blots. Antibody stripping from a Western blot was routinely performed following the procedures as described (*19*).

In Vitro Binding Assays for His-p67, GST-ERK1 (GST Pull Down), and ERK2. The binding of purified His-p67 and ERK1 or ERK2 was performed in the wash buffer mentioned above. For immobilization of His-p67 in Ni-NTA−agarose beads, 20 μL of slurry (50% beads, Qiagen) was washed two times with the wash buffer; purified His-p67 was added, and the binding was carried out at 4 °C for 1 h. Unbound His-p67 was removed by microcentrifugation, and GST-ERK1 or purified ERK2 was added into the beads containing 300−400 μL of wash buffer. As a control, a purified GST sample was used to detect nonspecific interaction with His-p67. The mixture was rotated at room temperature for 2 h, microcentrifuged, and washed extensively with ample amounts of wash buffer. To the beads was added 5× SDS-loading buffer, and the mixture was boiled for 10 min. After microcentrifugation, the supernatant was loaded on a 15% SDS−PAGE. The proteins from the gel were transferred to a nitrocellulose filter and detected with appropriate antibodies. The binding assays were repeated three times with similar results.

Activation of GST-ERK1 in Vitro. Purified GST-ERK1 was added into 300 μg of total proteins from C2C12 myoblasts and incubated at 30 °C for 30 min. Next 20 μL of glutathionine−agarose (50% beads, Sigma) was added into the mixture, and the resultant mixture was rotated at room temperature for 1 h. The mixture was then microcentrifuged and washed extensively with a washing buffer (25 mM Hepes, pH 7.6, 150 mM NaCl, and 0.1% NP-40). The GST-ERK1 bound to the beads was used for in vitro kinase assay.

In Vitro Phosphorylation of Myelin Basic Protein (MBP) by GST-ERK1 and ERK2. In a typical phosphorylation assay, 2 μg of MBP was phosphorylated by the bound activated GST-ERK1 or 6 ng of ERK2 in the presence of 50 mM Tris-HCl (pH 7.5), 10 mM $MgCl_2$, 1 mM EGTA, 2 mM DTT, 0.01% Brij 35, and 40 μM ATP. The reaction was initiated by adding 10 μCi of [γ-^{32}P]ATP (specific activity 3500 Ci/mmol, Amersham) and incubated at 30 °C for 30 min. The reactions were stopped by adding 5× SDS-loading dye and boiled for 10 min. The denatured samples were analyzed on a 15% SDS−PAGE followed by autoradiography or transferred to a nitrocellulose filter for Western blot analysis. The phosphorylation assays were repeated three times with similar results.

RESULTS

Fumagillin Treatment Increases the Stability of p67 in C2C12 Myoblasts. The effects of fumagillin treatment on endothelial cells have been demonstrated (*3*−*9*), but very little information is available regarding its effects on non-endothelial cells. We used mouse C2C12 myoblasts, and the IC_{50} value of fumagillin was determined to be 2.6 nM (data not shown). To examine whether the antiangiogenic drug, fumagillin, has any effect of the levels of p67, C2C12 myoblasts were treated with fumagillin for 24 and 36 h. During the treatments, the number of cycling cells decreased dramatically (data not shown). To detect the level of p67, we used two different types of polyclonal antibodies. One, which was obtained by immunizing mice with full-length p67 purified from rabbit reticulocytes, is named RD1. The other, which was obtained by immunizing mice with the downstream 108−480 amino acid segment of p67, is named RD2. Total cell lysates from fumagillin treated and untreated myoblasts were analyzed on a SDS−PAGE followed by immunoblotting with RD2 polyclonal antibodies (Figure 1A). In addition to the detection of p67, these antibodies detected a slower migrating protein running near 70 kDa (marked as "x"), whose level remains unchanged during fumagillin treatment and serves as an internal control. The faster migrating proteins detected by these polyclonal antibodies could be the degradation products of p67 (Figure 1A). The

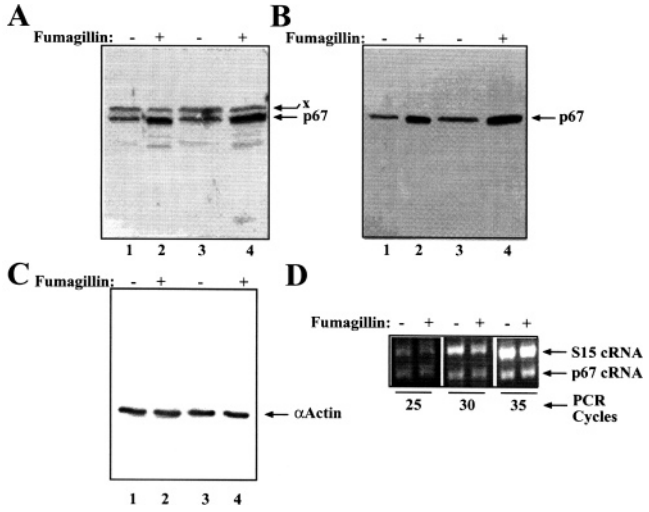

FIGURE 1: The levels of p67 increase in fumagillin-treated C2C12 myoblasts. C2C12 myoblasts were grown to 60% confluence and treated with fumagillin, the cells were harvested, lysates were made, and 100 μg of total protein samples was analyzed by a 15% SDS−PAGE followed by immunoblotting with polyclonal antibodies specific to the C-terminal 108−480 amino acid segment of p67 (A). The antibodies from the blot were stripped off and reprobed with polyclonal antibodies specific to p67 (B). The level of α-actin was measured as a loading control (C). Fumagillin treatment was done for 24 h (lane 2 in panels A−C) and 36 h (lane 4 in panels A−C). (D) Total RNA samples were isolated from fumagillin-treated and untreated cells; 2 μg of total RNA samples and two sets of primers (one pair for mRNA of S15 ribosomal protein and the other pair for an internal fragment of p67) were used for RT-PCR, and reaction mixtures were resolved by a 1.5% agarose gel. For a particular sample preparation, three PCR cycles (25, 30, and 35) were carried out to check the linearity of the identifications of cRNAs. To normalize the control S15 cRNA, double the sample amount was loaded in the lanes shown as fumagillin treatment. The size of the fragment for the internal control (S15 cRNA) is 361 nts, and the size of the fragment from the internal coding region of p67 is 240 nts.

antibodies from the blot were stripped off and reprobed with RD1 polyclonal antibodies (Figure 1B). These polyclonal antibodies do not detect the slower migrating protein and the faster migrating degraded protein products that could be detected by the RD2 polyclonal antibodies. These results suggest that the RD1 polyclonal antibodies could be specific to the N-terminal 1−107 amino acid segment of p67. The level of α-actin was measured for loading control of the above experiments (Figure 1C). These results demonstrate that the level of p67 increases in fumagillin-treated C2C12 myoblasts. The increased level of p67 in fumagillin-treated C2C12 myoblasts could be due to the increased levels of its mRNA or increased stability of the protein by fumagillin. To examine the first possibility, we measured the level of p67 mRNA through RT-PCR (Figure 1D). The results indicate that the level of p67 mRNA does not change in fumagillin-treated myoblasts. It is however consistent with repeated experiments that the levels of total mRNA and rRNA are at least 2−3-fold lower in fumagillin-treated C2C12 myoblasts as compared to untreated cells (data not shown), thus indicating an overall growth inhibition by fumagillin. Altogether, our data suggest that fumagillin treatment of C2C12 myoblasts causes an accumulation of p67.

Increased Levels of p67 in Fumagillin-Treated C2C12 Myoblasts Are Due to Its Low Turnover Rate. To examine

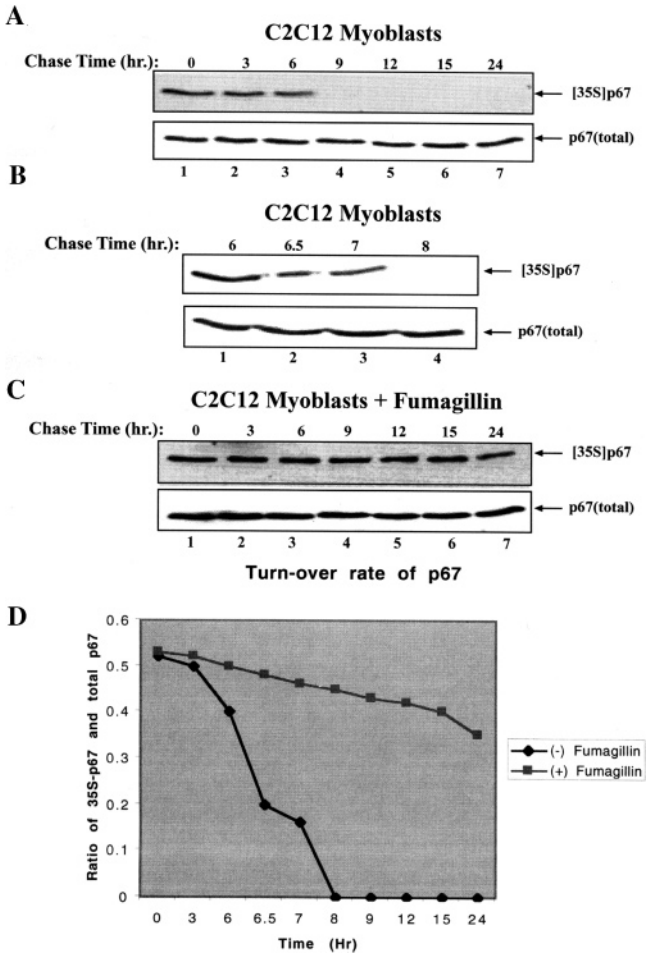

FIGURE 2: The turnover rate of p67 decreases in fumagillin-treated C2C12 myoblasts. Control C2C12 myoblasts (panels A and B) or fumagillin-treated myoblasts (C) were labeled with [^{35}S]methionine for 3 h; labeling medium was removed, and fresh growth medium was added to the cells. At different time intervals, the cells were harvested and lysates were prepared. 300 μg of total protein samples was used for immunoprecipitations by p67 polyclonal antibodies (A, upper panel). The IPs were analyzed on a 15% SDS−PAGE, transferred to a nitrocellulose filter, and exposed to X-ray films (panels A and B). To measure the total amounts of p67 protein, the same nitrocellulose filter was used for Western blot with p67 polyclonal antibodies (B). The above experiments were repeated three times, and band intensities were measured using NIH1.62 Imagequant software. A ratio of [^{35}S]methionine-labeled p67 and total p67 was calculated, and the average readings were plotted against chase time (D).

whether fumagillin treatment of C2C12 myoblasts increases the stability of p67, we performed pulse−chase experiments. C2C12 myoblasts were grown in growth medium and were treated with fumagillin for 24 h. Subsequently, treated and untreated cells were metabolically labeled with [^{35}S]methionine. The [^{35}S]methionine was removed from the culture medium by washing with growth medium, and the cells were allowed to grow further. At different time intervals, cells were harvested, and immunoprecipitation experiments were performed with polyclonal antibodies specific to p67 (Figure 2). The level of the radiolabeled p67 declines after 6 h of chase in control C2C12 cells (Figure 2A, upper panel), whereas this level remains unchanged until 15 h of chase and declines slightly at 24 h of chase in fumagillin-treated C2C12 myoblasts (Figure 2C, upper panel). The level of total p67 remains unchanged in control cells and in fumagillin-

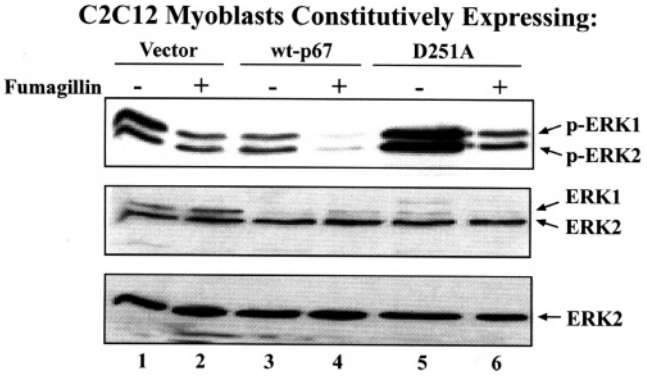

FIGURE 3: Phosphorylation of ERK1 and ERK2 kinases decreases in fumagillin-treated C2C12 myoblasts constitutively expressing wild-type p67 and the D251A mutant. C2C12 myoblasts constitutively expressing the EGFP vector or the EGFP fusions of wild-type p67 and the D251A mutant were treated with fumagillin; treated and untreated cells were harvested, and lysates were prepared. 100 μg of total protein samples was analyzed by a 15% SDS−PAGE followed by Western blot analyses with antibodies specific to p-ERKs 1 and 2 (upper panel), ERK1 and ERK2 (middle panel), and ERK2 (lower panel).

treated cells (Figure 2A,C, lower panels). To determine the exact time of declining levels of the radiolabed p67, we performed similar analysis as shown in Figure 2A, but in shorter time intervals after 6 h of chase (Figure 2B). On the basis of three independent experiments, we find that the time, where the radiolabeled p67 disappears in control cells, varies from 7 to 8 h after chase, indicating that the average turnover rate of p67 in C2C12 myoblasts is around 7.5 h and the half-life of p67 in C2C12 myoblasts is 6 h and 15 min (Figure 2D).

Constitutive Expression of p67 Decreases the Phosphorylation of ERK Kinases in Myoblasts. Fumagillin treatment of mammalian cells slows down growth (*5*). Growth of mammalian cells depends on the signal from the MAP-kinase pathway (*33*). When the MAP-kinase pathway is active, its downstream targets, extracellular signal-regulated kinases ERK1 and ERK2, are phosphorylated (*34*). This phosphorylation provides proliferative signals to the cells. To test whether the increased stability of p67 by fumagillin is involved in the modulation of phosphorylation of ERKs 1 and 2, we generated C2C12 cell lines constitutively expressing vector carrying enhanced green fluorescenct protein (EGFP) and its fusion with wild-type p67 and the D251A mutant. The D251 residue of p67 is one of the five conserved amino acid residues involved in metal ion binding (*27*) and possibly regulates the proteolytic activity of p67/MetAP2. The above cell lines were maintained in growth medium. When cell density reached to 60−70% confluence, fumagillin was added to the cultures, and the resultant cultures were grown for 24 h in a CO_2 incubator. Lysates from fumagillin-treated and untreated cells were analyzed for the levels of both ERK 1 and ERK2 and their phosphorylation (Figure 3). The phosphorylation of both ERK1 and ERK2 is lower in myoblasts constitutively expressing p67, and this level is quite higher in myoblasts constitutively expressing the D251A mutant as compared to control myoblasts constitutively expressing the expression vector. These cell lines, when treated with fumagillin, caused the phosphorylation levels of both ERK1 and ERK2 to drop significantly in both the vector-expressing and the wild-type p67-expressing

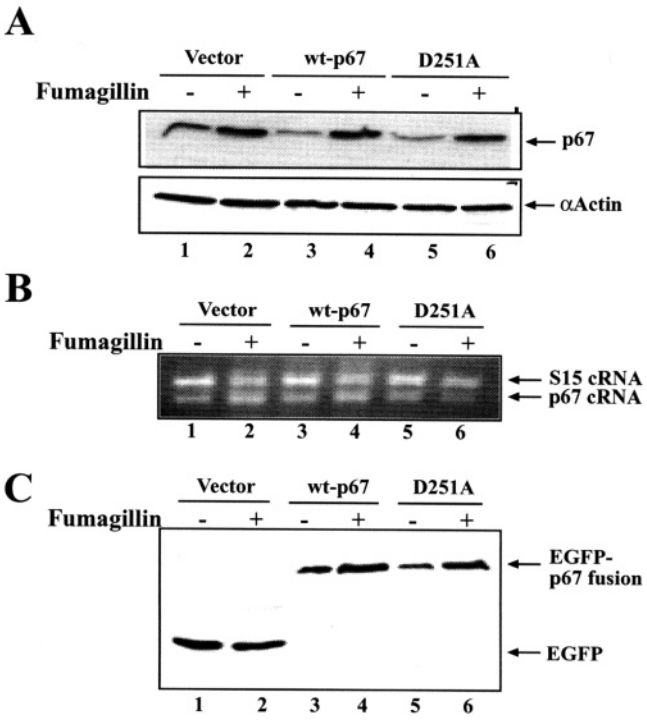

FIGURE 4: The level of p67 increases in fumagillin-treated C2C12 myoblasts constitutively expressing wild-type p67 and the D251A mutant. (A) Similar procedures as described in the legend to Figure 3 were followed for the analysis of the levels of p67 (upper panel) and α-actin (lower panel) using antibodies specific to those proteins. (B) Total RNA samples were isolated from the stable cell lines, and RT-PCR was carried out using two sets of primers: one set for the internal control (S15 cRNA) and the other set for the internal fragment of p67. A total of 30 PCR cycles was carried out. The DNA samples were resolved by an agarose gel and stained with ethidium bromide. 100 μg of the total protein samples from the above-mentioned lines was analyzed on a 15% SDS−PAGE followed by detection of proteins with a monoclonal antibody specific to EGFP (C). The EGFP fusions of wild-type p67 and the D251A mutant were detected as slower migrating bands.

myoblasts (upper panel). The phosphorylation level also dropped by severalfold in the D251A mutant-expressing cells (upper panel). Although the level of ERK2 remains unchanged (Figure 3, middle and lower panels), the level of ERK1 is considerably lower in myoblasts constitutively expressing wt p67 or the D251A mutant (Figure 3, middle panel). Fumagillin treatment of these latter cell lines does not change the level of ERK1. Considering the total amounts of ERK1 and ERK2 proteins in these cell lines, it is obvious that the phosphorylation of ERK1 in myoblasts constitutively expressing the D251A mutant is much greater than it is apparently seen in these gels. The C2C12 myoblasts constitutively expressing wt p67 and the D251A mutant expressed equal amounts of both fusion proteins (see below). Altogether, these data suggest that the phosphorylation of both ERK1 and ERK2 is considerably inhibited by fumagillin treatment.

Constitutive Expression of p67 or the D251A Mutant Does Not Change the Fumagillin-Induced Stability of p67. To examine whether the constitutive expression of wt p67 or the D251A mutant interferes with the level of endogenous p67, we determined the level of endogenous p67 on a Western blot in whole cell lysates prepared from cells constitutively expressing the expression vector, wt p67, and the D251A mutant (Figure 4A). We find that the level of

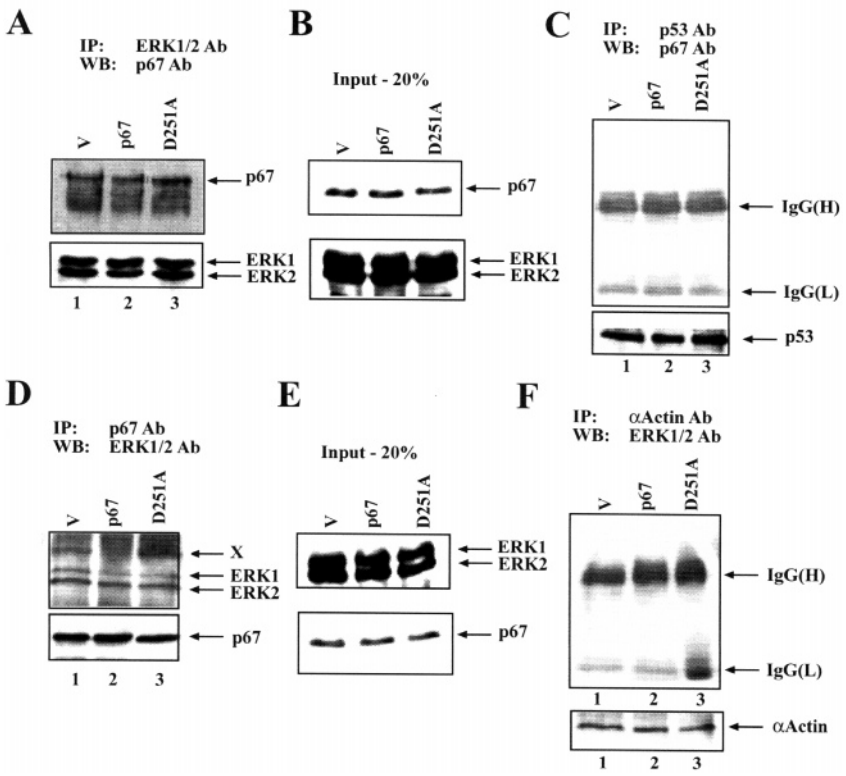

FIGURE 5: p67 binds to ERK1 and ERK2. Mouse C2C12 myoblasts constitutively expressing the EGFP vector and the EGFP fusions of wild-type p67 and the D251A mutant were grown, and cell lysates were prepared. 300 μg of the total protein samples was used for immunoprecipitation experiments with rabbit polyclonal antibodies specific to ERK1/2 (A), a monoclonal antibody specific to p53 (C), mouse polyclonal antibodies specific to p67 (D), and a monoclonal antibody specific to α-actin (F). Immunoprecipitates from experiments in panels A and C were analyzed on a 15% SDS−PAGE followed by detection of proteins with mouse polyclonal antibodies specific to p67 (A and C, upper panels), rabbit polyclonal antibodies specific to ERK1 and ERK2 (A, lower panel), and a monoclonal antibody specific to p53 (C, lower panel). Likewise, immunoprecipitates from experiments in panels D and F were analyzed on a 15% SDS−PAGE followed by detection of proteins with rabbit polyclonal antibodies specific to ERK1/2 (D and F, upper panels), mouse polyclonal antibodies specific to p67 (D, lower panel), and a monoclonal antibody specific to α-actin (F, lower panel). 20% of the input proteins used for immunoprecipitation experiments in panels A and D were probed with mouse polyclonal antibodies specific to p67, ERK1, and ERK2, and the results are shown in panels B and E. Proteins corresponding to IgG heavy and light chains are indicated by IgG(H) and IgG(L), respectively. The slower migrating protein, marked as X, is detected by antibodies specific to ERKs 1 and 2 only in cell lysates from the vector or the D251A mutant. In panels A and D, the immunoprecipitated IgGs are not detected by the secondary antibodies because whole IgGs are raised in different species.

endogenous p67 is low in untreated cells (lanes 1, 3, and 5) and that this level increases by 3−4-fold in fumagillin-treated cells (lanes 2, 4, and 6), which are consistent with our previous experiments shown earlier. Since this increased level could be due to the increased levels of p67 mRNA, we measured the p67 mRNA level from the above cell lines and found that the message level of p67 remains unchanged when we compared the ratio of control S15 cRNA and p67 cRNA (Figure 4B). We also determined the turnover rate of p67 in these cell lines by pulse−chase experiments and noticed that p67 is stable for at least 24 h in these cells treated with fumagillin (data not shown). As a control experiment, we measured the levels of EGFP and its fusion with wild-type p67 and the D251A mutant in fumagillin-treated and untreated cells from the above lines. The levels of the exogenously expressed fusion proteins are 2−3-fold higher in fumagillin-treated cells as compared to untreated cells (compare lanes 3 and 5 with lanes 4 and 6 in Figure 4C). The artificial promoter controls the synthesis of EGFP mRNA, the EGFP fusions of p67, and the D251A mRNAs. Therefore, we do not see any change in the mRNA levels of p67 or its mutant, D251A, in fumagillin-treated cells. However, the stability of these proteins is increased due to the binding of fumagillin. Altogether, these results suggest that fumagillin increases the stability of p67 in myoblasts by decreasing the turnover rate of the protein.

p67 Binds to ERK1 and ERK2 in C2C12 Myoblasts. The studies mentioned above demonstrate that p67 interferes with the phosphorylation of the ERKs in C2C12 myoblasts. To examine whether this is due to the binding between these proteins, we performed immunoprecipitation experiments in control C2C12 myoblasts constitutively expressing EGFP or in cell lines constitutively expressing the EGFP fusion of wild-type p67 and the D251A mutant (Figure 5). In a first set of experiments, immunoprecipitations were done with rabbit polyclonal antibodies specific to ERK1 and ERK2 (Figure 5A). In a control experiment, the immunoprecipitation was done by mouse monoclonal antibodies specific to p53 (Figure 5C). Both blots were then probed with mouse polyclonal antibodies specific to p67 (Figure 5A,C). The first blot was reprobed with polyclonal antibodies specific to ERK1 and ERK2 (Figure 5A, lower panel), and the second blot was reprobed with a monoclonal antibody specific to p53 (Figure 5C, lower panel). To estimate the percentage of material immunoprecipitated, 20% of the input samples were analyzed for the levels of p67 (Figure 5B, upper panel) and ERK1 and ERK2 (Figure 5B, lower panel). To verify these interactions further, we performed immunoprecipitation

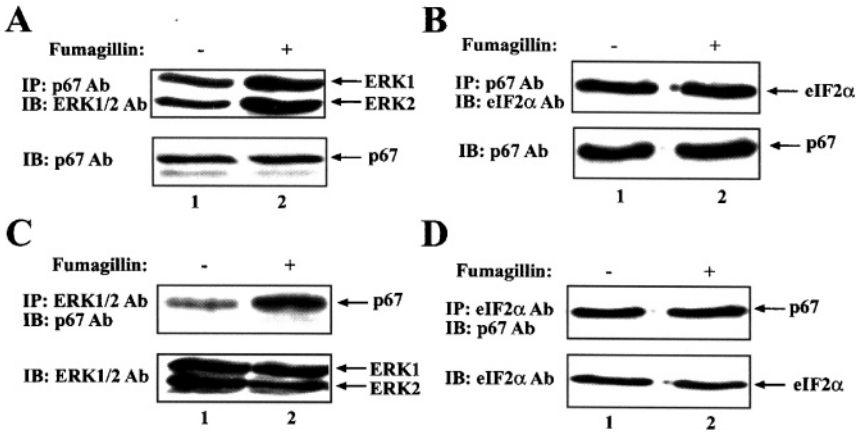

FIGURE 6: The binding affinity of p67 with ERKs 1 and 2 increases and that with eIF2α remains unchanged in fumagillin-treated mouse C2C12 cells. Total cell extracts from fumagillin treated and untreated C2C12 cells were analyzed for binding between p67 and ERKs 1 and 2 by immunoprecipitation assays with polyclonal antibodies specific to p67 (A and B), and the IPs were analyzed on a 15% SDS−PAGE followed by immunoblots to detect ERKs 1 and 2 (A), eIF2α (B), and p67 (A and B, lower panel). Similar immunoprecipitation assays were performed with polyclonal antibodies specific to ERK1 and ERK2 (C) and to eIF2α (D). The IPs were analyzed on a 15% SDS−PAGE followed by immunoblots to detect p67 (C and D), ERK1 and ERK2 (C, lower panel), and eIF2α (D, lower panel). These experiments were repeated three times with similar results.

experiments with mouse polyclonal antibodies specific to p67 (Figure 5D) and with mouse polyclonal antibodies specific to α-actin (Figure 5F). The immunoprecipitates were analyzed on a SDS−PAGE followed by Western blots with rabbit polyclonal antibodies specific to ERK1/2 (Figure 5D,F). The antibodies were stripped off and reprobed with mouse polyclonal antibodies specific to p67 (Figure 5D, lower panel) and a mouse monoclonal antibody specific to α-actin (Figure 5F, lower panel). To estimate the percentage of immunoprecipitations, 20% of the input samples were analyzed on Western blots for the levels of ERKs 1 and 2 (Figure 5E, upper panel) and p67 (Figure 5E, lower panel). Our data show that p67 binds to ERKs 1 and 2 and the D251A mutant does not have any effect on this interaction. We, however, expected to detect an increased level of binding between p67 and ERKs 1 and 2 in p67-expressing cells. In contrast, we detected almost an equal level of binding in the above cell line as compared to control cells constitutively expressing EGFP alone (lane 1 in panels A and D of Figure 5). As we compare the percentage efficiency of the immunoprecipitations with that of the input, we find that we can precipitate p67 by ERKs 1 and 2 antibodies only 5−10% of the input samples (compare results in Figure 5A with those in Figure 5B) and ERKs 1 and 2 by p67 antibodies only 3−5% of the input (compare results in Figure 5D with those in Figure 5E). This may provide a possible explanation why we have not detected increased levels of ERKs 1 and 2 during precipitation by p67 in p67-expressing cells. A protein, marked "X", shows cross-reactivity with antibodies specific to ERKs 1 and 2 and is also pulled down by p67. Its identity is not known at present. Altogether, these results demonstrate that the binding between p67 and ERK1 and ERK2 and the D251A mutant apparently has no effect on this interaction.

Binding Affinity of p67 and ERKs 1 and 2 Increases and That with eIF2α Remains Unchanged in Fumagillin-Treated C2C12 Myoblasts. Since the level of p67 increases in fumagillin-treated mouse myoblasts due to its increased stability, we wanted to test whether p67's affinity to the ERKs changes in fumagillin-treated cells. Cell extracts from fumagillin-treated C2C12 myoblasts were used to immunoprecipitate either ERKs 1 and 2 or eIF2α with polyclonal antibodies specific to p67 (Figure 6A,B). Similarly, p67 was coprecipitated with ERKs 1 and 2 and eIF2α using their specific antibodies (Figure 6C,D). The IPs were analyzed to detect ERKs 1 and 2, eIF2α, and p67 on Western blots with polyclonal antibodies specific to these proteins. Our data demonstrate that the binding affinity of p67 to ERKs 1 and 2 and vice versa increases when cells are treated with fumagillin.

The 108−480 Amino Acid Segment of p67 Binds to ERKs 1 and 2. The entire p67 protein could be divided into two segments: the N-terminal 1−107 amino acid segment and the downstream 108−480 amino acid segment (*10*). To examine which segment of p67 binds to ERKs 1 and 2, we performed immunoprecipitation assays with C2C12 cell extracts. These cell extracts were obtained from transiently transfected cells. The plasmids used for transfection were either Myc epitope-tagged expression plasmids encoding wild-type p67 and its above two segments or Flag epitope-tagged expression plasmids encoding ERK1 and ERK2. The immunoprecipitates from Myc monoclonal antibody were analyzed with Flag monoclonal antibody to detect which Flag fusion protein was coprecipitated (Figure 7A). Similarly, immunoprecipitates from Flag monoclonal antibody were analyzed with Myc monoclonal antibody to detect which Myc fusion protein was coprecipitated (Figure 7B). Immunoprecipitates were also analyzed for the same antibodies to determine the success of the immunoprecipitation reactions (Figure 7A,B, lower panels). We noticed that both ERK1 and ERK2 coprecipitated with wild-type p67 and the 108−480 amino acid segment but not with the N-terminal 1−107 amino acid segment. In addition to the binding of ERKs 1 and 2, we noticed a somewhat lesser binding between p67 and ERK2 as compared to ERK1 (compare lanes 3 and 4 and lanes 5 and 6 in the upper panels in Figure 7A,B). In reciprocal experiments we further verified these results. Altogether, these results suggest that the 108−480 amino acid segment of p67 is required for binding with ERKs 1 and 2.

p67 Binds Directly to ERK1 and Inhibits Its Activity in Vitro. To examine whether the binding between p67 and ERK1 is direct, we performed a GST pull-down assay where

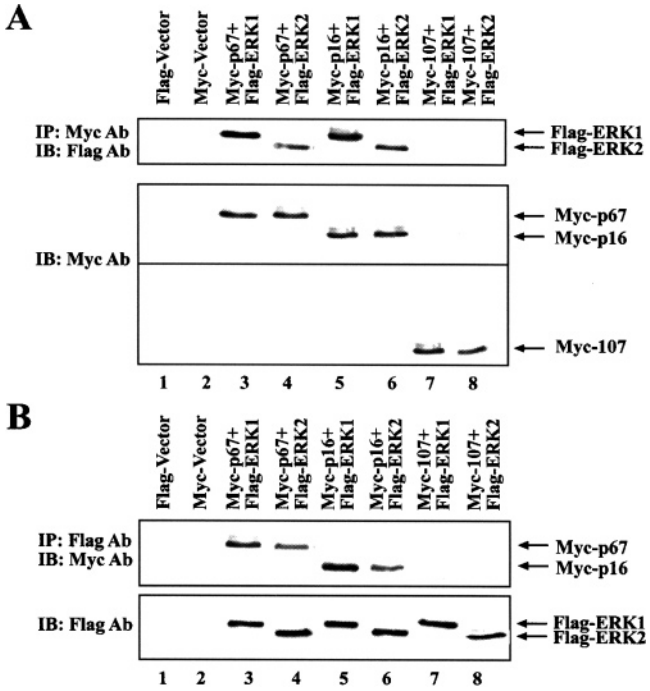

FIGURE 7: The 108−480 amino acid segment of p67 binds to ERKs 1 and 2. C2C12 cells were transiently transfected with the expression vectors Flag and Myc (lanes 1 and 2) alone and with pairwise combinations of Myc-p67 and Flag-ERK1 (lane 3), Myc-p67 and Flag-ERK2 (lane 4), Myc-p16 and Flag-ERK1 (lane 5), Myc-p16 and Flag-ERK2 (lane 6), Myc-107 and Flag−ERK1 (lane 7), and Myc-107 and Flag-ERK2 (lane 8). 42 h after transfection, cells were harvested, and immunoprecipitation experiments were performed with a monoclonal antibody specific to Myc (A) and to Flag (B). The IPs were analyzed on a 15% SDS−PAGE followed by immunoblots with a monoclonal antibody specific to Flag (A, upper panel) and to Myc (B, upper panel). The IPs were also analyzed on immunoblots to detect the immunoprecipitated Myc fusions (A, middle and lower panels) and Flag fusions (B, lower panel). These experiments were repeated two times with similar results. During ECL analysis, signals from the IgGs were blocked by removing the appropriate portion of the blot corresponding to molecular mass markers 25 kDa (IgG, light chain) and 50 kDa (IgG, heavy chain). The approximate molecular masses of Myc-p67, Myc-p16, and Myc-107 are 68, 54, and 12 kDa, respectively.

either GST (lane 2, Figure 8A) or GST-ERK1 (lane 3) was bound to glutathione−agarose; His-p67 was added into the beads. Bound proteins with the beads were further analyzed on Western blots with polyclonal antibodies specific to p67 (Figure 8A, upper panel), and the input His-p67 was detected with the same antibody (Figure 8A, lower panel). To detect the same interactions in the other direction, His-p67 was bound to Ni-NTA−agarose beads. To these beads was added GST (lane 2, Figure 8B) or GST-ERK1 (lane 3), and polyclonal antibodies specific to ERK1 were used to detect proteins bound in the beads by Western blots. Input His-p67 bound to the beads was detected with polyclonal antibodies specific to p67 (Figure 8B, lower panel). To rule out the possibility that GST-ERK1 can bind to Ni-NTA−agarose beads nonspecifically, we incubated the beads with GST-ERK1 and detected no binding (Figure 8B, lane 3). Altogether, these results demonstrate direct and specific interactions between p67 and ERK1. To examine whether this binding affects the activity of ERK1, we performed an in vitro phosphorylation assay using myelin basic protein (MBP) as a substrate and artificially activated ERK1 (Figure 8C). Activated ERK1 phosphorylates MBP (lane 2), and this phosphorylation is completely inhibited by p67 (lane 4). MBP does not autophosphorylate (lane 1) and p67 cannot phosphorylate MBP (lane 3). Taken together, these results suggest that p67 binds and inhibits the activity of ERK1.

p67 Binds ERK2 Directly and Inhibits Its Activity in Vitro. To test for the binding between p67 and ERK2, purified His-p67 was bound to the Ni-NTA−agarose beads and kinase-active purified ERK2 was added into the binding buffer. After binding, beads were analyzed for bound proteins with a monoclonal antibody specific to ERK2 (Figure 9A). An unrelated GST protein was also used to test for nonspecific binding (lane 2). The input His-p67 was detected by polyclonal antibody specific to p67 (Figure 9A, lower panel). To rule out the possibility that the purified ERK2 can bind to Ni-NTA−agarose beads nonspecifically, we incubated the beads with ERK2 and detected no binding (Figure 9A, lane 3). Our results thus show that ERK2 binds to p67 specifically. To examine whether p67 inhibits the activity of ERK2, we performed an in vitro phosphorylation assay using ERK2 as the kinase and MBP as the substrate. We found that ERK2 phosphorylates MBP (lane 2) and this phosphorylation could be inhibited significantly by p67 (lane 4). MBP does not autophosphorylate (lane 1) and p67 cannot phosphorylate MBP (lane 3). Altogether, these data suggest that p67 binds and inhibits the activity of ERK2.

DISCUSSION

Solid tumors need active angiogenesis to provide nutrients and growth factors. The antiangiogenic inhibitors inhibit growth factor-mediated endothelial cell growth. Among these inhibitors, fumagillin, AGM-1470/TNP470, and ovalicin are natural products (*35*), which inhibit the growth of endothelial cells by arresting cells at the G_1/S and G_2/M phases of the cell cycle (*3*, *4*, *8*, *9*). The cellular target for fumagillin is MetAP2, and not MetAP1, although both proteins share significant sequence identities at their C-terminal amino acid sequences. The MetAP2 and p67 are the same proteins. p67 protects the α-subunit of eIF2 from phosphorylation by its kinases (*11*−*14*, *17*−*21*). On the basis of this evidence, it is now considered that p67 is a bifunctional protein (*10*, *37*). The N-terminal amino acid sequences of MetAP1 and MetAP2 differ considerably (*24*). This raises the possibility that the N-terminus of p67/MetAP2 may have additional binding site(s) for fumagillin in addition to the H231 residue. The MetAPs remove the N-terminal methionine, and myristoyltransferase adds the myristoyl group at the glycine residue. The latter modification targets the protein to the membrane for its activity. It is not clear yet what that target protein is. To determine the molecular mechanisms of growth inhibitory effects of fumagillin in endothelial cells, Abe et al. found that the fumagillin derivative AGM-1470 inhibits activation of cdks and phosphorylation of the retinoblastoma gene product, pRb, but not protein tyrosyl phosphorylation or protooncogene expression in vascular endothelial cells (*8*). Later, Zhang et al. found that cell cycle inhibition by the antiangiogenic agent TNP-470 is mediated by p53 and $p21^{WAF1/CIP1}$ (*36*).

Since the mammalian cell cycle is regulated by the availability of nutrients and growth factors, we suspected that the MAP kinase pathway might be involved in cell growth inhibition by the treatment of fumagillin. We tested

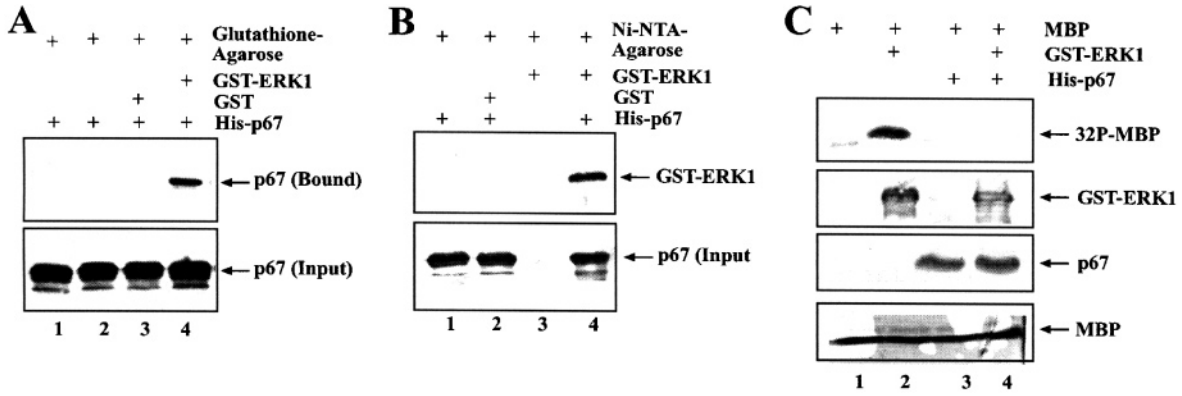

FIGURE 8: p67 binds to ERK1 and inhibits its activity in vitro. (A) GST or GST-ERK1 proteins (1 μg each) was bound to glutathione−agarose, and 1.2 μg of purified His-p67 was added to the beads. As a duplicate control, the same amount of His-p67 was added to the beads alone (lanes 1 and 2). After extensive washing, samples from the beads were analyzed on a 15% SDS−PAGE followed by detection of the p67 protein by its polyclonal antibodies (upper panel). Input p67 is shown in the lower panel. (B) The Ni-NTA−agarose beads were washed, and His-p67 (1.2 μg) was bound to the beads (lanes 1, 2, and 4). To these beads was added either GST (lane 2) or GST-ERK1 (lane 4), and the resultant solution was allowed to bind at room temperature. A similar binding experiment was performed with GST-ERK1 and Ni-NTA−agarose beads (lane 3). After extensive washing, the beads were analyzed on a 15% SDS−PAGE followed by detection of ERK1 with its polyclonal antibodies (B). Input p67 is shown in the lower panel. (C) 2 μg of myelin basic protein (MBP) was phosphorylated by the activated GST-ERK1 in the presence (lane 4) and absence (lane 2) of purified His-p67. Control experiments are shown in lanes 1 and 3. Phosphorylated proteins were analyzed on 15% SDS−PAGE and autoradiographed. The proteins from the gel were transferred to a nitrocellulose filter. GST-ERK1 and His-p67 proteins were detected with respective polyclonal antibodies. MBP was detected by Coomassie staining of the gel after autoradiography.

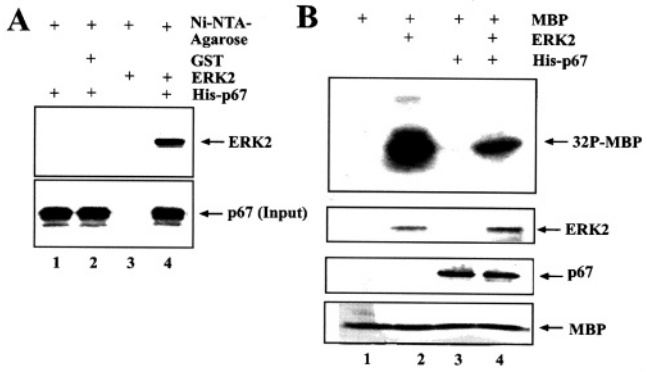

FIGURE 9: p67 binds to ERK2 and inhibits its activity in vitro. (A) 1.2 μg of purified His-p67 was bound to the Ni-NTA−agarose beads (lanes 1, 2, and 4); 1 μg of GST, an unrelated protein (lane 2), or 60 ng of purified ERK2 proteins (lane 4) was added to the p67-bound beads. As an additional control, Ni-NTA−agarose beads were incubated with ERK2 (lane 3). After extensive washing, samples from the beads were analyzed on a 15% SDS−PAGE followed by detection of ERK2 protein by its monoclonal antibody (upper panel). Input p67 is shown in the lower panel. (B) 2 μg of myelin basic protein (MBP) was phosphorylated by the activated ERK2 in the presence (lane 4) and absence (lane 2) of purified His-p67. Control experiments are shown in lanes 1 and 3. Phosphorylated proteins were analyzed on a 15% SDS−PAGE and autoradiographed. The proteins from the gel were transferred to a nitrocellulose filter. ERK2 and His-p67 proteins were detected with their respective monoclonal and polyclonal antibodies. MBP was detected by Coomassie staining of the gel after autoradiography.

the fumagillin sensitivity of C2C12 myoblasts, which originated from mouse thigh muscles. The IC_{50} of fumagillin in C2C12 cells is 2.6 nM (this study), and this number is very close to what was found in endothelial cells (*37*, *38*). C2C12 myoblasts proliferate in serum-rich medium and undergo fusion into myotubes when a confluent culture is grown in low serum medium (*39*). This will allow for the examination of the morphological changes of C2C12 myoblasts after treatment with growth inihibitors such as fumagillin. Fumagillin covalently binds to p67/MetAP2 (*27*). It stabilizes the p67 protein (Figure 1) by decreasing its turnover rate (Figure 2). Growth and proliferation signals are provided by the growth factors, which use the MAP kinase pathway to transduce signals into the nucleus. Our in vitro and ex vivo (cell culture) studies provide evidence that p67 binds to eIF2 and modulates the phosphorylation of eIF2α (*21*). To understand the molecular details of how the growth inhibitory signal due to eIF2α phosphorylation is counterbalanced by the growth stimulatory signal provided by the phosphorylation of ERKs 1 and 2, we examined the effects on phosphorylation of these kinases by p67. We find that p67 inhibits the phosphorylation of ERKs 1 and 2 (Figures 3, 8, and 9) and this is mediated by binding to both ERK1 and ERK2 (Figures 5 and 6). The 108−480 amino acid segment of p67 is sufficient for binding (Figure 7). Among several mechanisms of cell growth inhibition by fumagillin, the underlying mechanism in this study shows a direct link between the action of fumagillin and the regulation of mammalian cell growth and proliferation by its cellular target, p67. We are currently determining the binding domains of p67 and ERKs 1 and 2 and their possible roles in MAP kinase-mediated signaling pathways.

The X-ray crystallographic study of the fumagillin−MetAP2/p67 complex identifies the H231 residue as the site for fumagillin binding. The MetAP2/p67 used in this study was purified from baculovirus (*27*). We recently purified His-p67 from baculovirus-infected Sf21 cells, and when stored in −80 °C for a period of few weeks, we detected a significant level of degradation (data not shown). Consistent with this finding is the report by Yang et al. that shows that the N-terminal 1−107 amino acid segment is removed when the purified MetAP2 sample was kept at 4 °C for 5−7 days (*40*). In our cell culture studies, we detected a low level of degradation of p67 by using RD2 polyclonal antibodies but not by using RD1 polyclonal antibodies (Figure 1A,B and data not shown), indicating that the fragments of p67 that are detected are from its C-terminal region. This study also provides evidence that fumagillin binding to p67 increases

its stability (Figure 1), possibly by inhibiting the autoproteolytic degradation of this protein. Then what causes its low level of degradation when mammalian cells were treated with fumagillin is not clear at present. It is possible that p67 may have additional catalytic sites that are not inhibited by fumagillin.

p67 binds to eIF2α (*14*, *41*) and ERKs 1 and 2 (this study). The N-terminal amino acid sequences of p67 are involved in binding to eIF2α (*14*), whereas the downstream 108−480 amino acid segment of p67 binds to ERKs 1 and 2. This raises the possibility that two complexes, p67/eIF2α and p67/ERKs, exist in mammalian cells or a ternary complex with eIF2, p67, and ERKs exists. The p67/eIF2α complex will allow mammalian cell growth by protecting eIF2α from phosphorylation by eIF2α-specific kinases, and the p67/ERKs complex downregulates the excessive growth-promoting signal mediated by the ERK MAP-kinase mediated pathway. Consistent with the first possibility is the finding that fumagillin treatment of C2C12 cells increases the affinity of p67 to ERKs 1 and 2 without changing the binding affinity for eIF2α (Figure 6). The later results are in agreement with the previous report by Griffith et al., that fumagillin binding to p67 does not affect eIF2α phosphorylaiton (*29*); rather, it slows down cell growth by inhibiting the phosphorylation of ERKs 1 and 2 (this study). Our recent study indicates that the O-glycosylation at the $_{60}$SGTS$_{63}$ site enhances the binding of p67 to eIF2α (*14*). This therefore suggests that fumagillin treatment of C2C12 myoblasts possibly does not alter glycosylation of p67.

The proteolytic activity of p67/MetAP2 depends on divalent metal binding, and the five conserved amino acid residues D251, D262, H331, E364, and E459 are involved in this process (*10*). The mutation of D251 to alanine increases phosphorylation of ERKs 1 and 2 in C2C12 cells, and this phosphorylaiton is inhibited by fumagillin due to the stabilization of p67 (Figures 3 and 4). This indicates the possibility that the fumagillin binding site(s) of p67 is (are) not affected by the D251A mutation; rather, the D251 residue modulates the phosphorylation of ERKs 1 and 2. Consistent with this is the fact that the 108−480 amino acid segment of p67 binds to both ERKs 1 and 2 (Figure 7). C2C12 cells constitutively expressing wild-type p67 and its D251 mutant show lower levels of ERK1 but higher levels of its phosphorylation in both wild-type and D251A-expressing cells (Figure 3). The molecular details of this observation are not clear at present. The intriguing possibility could be that ERK1 is unstable or its synthesis is being modulated in the above cell lines.

We noticed earlier that the N-terminal 1−97 amino acid residues show increased levels of protection of eIF2α phosphorylation when constitutively expressed in rat tumor hepatoma cells (*11*). An intriguing possibility is that p67 generates this fragment by its endoproteolytic activity and the effective concentration of this fragment could determine the basal cellular level of eIF2α phosphorylation. Indeed, we have detected at least two fragments running near 17 and 5 kDa in cycling C2C12 myoblasts, and these fragments are quite stable (data not shown). Previous reports indicated that the three-dimensional fold of MetAP2 is very similar to serine proteases (*25*), a subset of which uses the lysine/arginine residues as their cleavage sites. The N-terminus of p67 has two lysine-rich domains separated by an acidic residue-rich domain (*10*). If p67 is cleaved endoproteolytically at these sites, it will generate fragments very similar to 17 and 5 kDa. It is, therefore, conceivable that the highly conserved D251 amino acid residue may play an important role in this proteolytic process. In addition to the D251 residue, two other conserved amino acid residues (H331 and E364) are also involved in the regulation of eIF2α phosphorylation during serum-starved conditions and serum-restoration conditions (*41*). This may provide a possible link between the growth stimulatory signals and growth inhibitory signals that are modulated by p67. In this study, we find novel observations that mouse C2C12 myoblasts are sensitive to the anticancer drug, fumagillin, which inhibits the growth of myoblasts by inhibiting the phosphorylation of ERKs 1 and 2, and the stability of p67 plays an important role in this process. We are currently determining what roles p67 plays in the regulation of other MAP kinase signaling pathways including the TGFβ-signaling pathway.

REFERENCES

1. Folkman, J. (1996) Fighting cancer by attacking its blood supply, *Sci. Am. 275*, 150−153.
2. Hanahan, D., and Folkman, J. (1996) Patterns and emerging mechanisms of the angiogenesis switch during tumorigenesis, *Cell 86*, 353−364.
3. Kusaka, M., Sudo, K., Matsutani, E., Kozai, Y., Marui, S., Fujita, T., Ingber, D., and Folkman, J. (1994) Cytostatic inhibition of endothelial cell growth by the angiogenesis inhibitor TNP-470 (AGM-1470), *Br. J. Cancer 69*, 212−216.
4. Antoine, N., Greimers, R., DeRoanne, C., Kusaka, M., Heinen, E., Simar, L. J., and Castronovo, V. (1994) AGM-1470, a potent angiogenesis inhibitor, prevents the entry of normal but not transformed endothelial cells into the G1 phase of the cell cycle, *Cancer Res. 54*, 2073−2076.
5. Ingber, D., Fujita, T., Kishimoto, S., Sudo, K., Kanamaru, T., Brem, H., and Folkman, J. (1990) Synthetic analogues of fumagillin that inhibit angiogenesis and suppress tumour growth, *Nature 348*, 555−557.
6. Castronovo, V., and Belotti, D. (1996) TNP-470 (AFM-1470): Mechanisms of action and early clinical development, *Eur. J. Cancer 32A*, 2520−2527.
7. Turk, B. E., Griffith, E. C., Wolf, S., Biemann, K., Chang, Y. H., and Liu, J. O. (1999) Selective inhibition of amino-terminal methionine processing by TNP-470 and ovalicin in endothelial cells, *Chem. Biol. 6*, 823−833.
8. Abe, J., Zhou, W., Takuwa, N., Taguchi, J., Kurokawa, K., Kumada, M., and Takuwa, Y. (1994) A fumagillin derivative angiogenesis inhibitor, AGM-1470, inhibits activation of cyclin-dependent kinases and phosphorylation of retinoblastoma gene product but not protein tyrosyl phosphorylation or protooncogene expression in vascular endothelial cells, *Cancer Res. 54*, 3407−3412.
9. Hori, A., Ikeyama, S., and Sudo, K. (1994) Suppression of cyclin D1 mRNA expression by the angiogenesis inhibitor TNP-470 (AGM-1470) in vascular endothelial cells, *Biochem. Biophys. Res. Commun. 204*, 1067−1073.
10. Datta, B. (2000) MAPs and POEP of the roads from prokaryotic to eukaryotic kingdoms *Biochimie 82*, 95−107.
11. Datta, R., Choudhury, P., Bhattacharya, M., Leon, F. S., Zhou, Y., and Datta, B. (2001) Protection of translation initiation factor eIF2 phosphorylation correlates with eIF2-associated glycoprotein p67 levels and requires the lysine-rich domain I of p67, *Biochimie 83*, 919−931.
12. Datta, R., Tammali, R., and Datta, B. (2003) Negative regulation of the protection of eIF2α phosphorylation activity by a unique acidic domain present at the N-terminus of p67, *Exp. Cell Res. 283*, 237−246.
13. Datta, B., and Datta, R. (2003) Mutation at the acidic residue-rich domain of eukaryotic initiation factor 2-associated glycoprotein, p67 increases the protection of eIF2α phosphorylation during heat-shock, *Arch. Biochem. Biophys. 413*, 116−122.
14. Datta, R., Choudhury, P., Ghosh, A., and Datta, B. (2003) A glycosylation site, $_{60}$SGTS$_{63}$ of p67 is required for its ability to

regulate the phosphorylation and activity of eukaryotic initiation factor 2α, *Biochemistry 42*, 5453−5460.
15. Hershey, J. W. B. (1991) Translational control in mammalian cells, *Annu. Rev. Biochem. 60*, 717−755.
16. Merrick, W. C., and Hershey, J. W. B. (2000) Pathway and mechanism of initiation of protein synthesis, in *Translational Control of Gene Expression* (Hershey, J. W. B., Mathews, M. B., and Sonenberg, N., Eds.) pp 33−88, Cold Spring Harbor Laboratory Press, Cold Spring Harbor, NY.
17. Datta, B., Chakrabarti, D., Roy, A. L., and Gupta, N. K. (1988) Roles of a 67kDa polypeptide in protein synthesis inhibition in heme-deficient reticulocyte lysates, *Proc. Natl. Acad. Sci. U.S.A. 85*, 3324−3328.
18. Datta, B., Datta, R., Mukherjee, S., and Zhang, Z. (1999) Increased phosphorylation of eukaryotic initiation factor 2α at the G_2/M boundary in human osteosarcoma cells correlates with deglycosylation of p67 and a decreased rate of protein synthesis, *Exp. Cell Res. 250*, 223−230.
19. Datta, B., and Datta, R. (1999) Induction of apoptosis due to lowering the level of eukaryotic initiation factor 2-associated protein, p67, from mammalian cells by antisense approach, *Exp. Cell Res. 246*, 376−383.
20. Datta, B., Ray, M. K., Chakrabarti, D., Wylie, D. E., and Gupta, N. K. (1989) Glycosylation of eukaryotic peptide chain initiation factor 2 (eIF-2)-associated 67-kDa polypeptide (p^{67}) and its possible role in the inhibition of eIF-2 kinase-catalyzed phosphorylation of the eIF-2α-subunit, *J. Biol. Chem. 264*, 20620−20624.
21. Ray, M. K., Chakraborty, A., Datta, B., Chattopadyay, A., Saha, D., Bose, A., Kinzy, T. G., Hileman, R. E., Merrick, W. C., and Gupta, N. K. (1993) Characterization of the eukaryotic initiation factor 2 associated 67-kDa polypeptide, *Biochemistry 32*, 5151−5159.
22. Wu, S., Gupta, S., Chatterjee, N., Hileman, R. E., Kinzy, T. G., Denslow, N. D., Merrick, W. C., Chakrabarti, D., Osterman, J. C., and Gupta, N. K. (1993) Cloning and characterization of complementary DNA encoding the eukaryotic initiation factor 2-associated 67-kDa protein (p^{67}), *J. Biol. Chem. 268*, 10796−10801.
23. Li, X., and Chang, Y.-H. (1995) Molecular cloning of a human complementary DNA encoding an initiation factor 2-associated protein (p^{67}), *Biochim. Biophys. Acta 1260*, 333−336.
24. Li, X., and Chang, Y.-H. (1995) Amino-terminal protein processing in *Saccharomyces cerevisiae* is an essential function that requires two distinct methionine aminopeptidases, *Proc. Natl. Acad. Sci. U.S.A. 92*, 2357−2361.
25. Bazan, J. F., Weaver, L. H., Roderick, S. L., Huber, R., and Matthews, B. W. (1994) Sequence and structure comparison suggest that methione aminopeptidase, prolidase, aminopeptidase P, and creatinase share a common fold, *Proc. Natl. Acad. Sci. U.S.A. 91*, 2473−2477.
26. Roderick, S. L., and Matthews, B. W. (1993) Structure of the cobalt-dependent methionine aminopeptidase from *Escherichia coli*: a new type of proteolytic enzyme, *Biochemistry 32*, 3907−3912.
27. Liu, S., Widom, J., Kemp, C. W., Crews, C. M., and Clardy, J. (1998) Structure of human methionine aminopeptidase-2 complexed with fumagillin, *Science 282*, 1324−1327.
28. Griffith, E. C., Su, Z., Niwayama, S., Ramsay, C. A., Chang, Y.-W., Wu, Z., and Liu, J. O. (1998) Molecular recognition of angiogenesis inhibitors fumagillin and ovalicin by methionine aminopeptidase 2, *Proc. Natl. Acad. Sci. U.S.A. 95*, 15183−15188.
29. Griffith, E. C., Su, Z., Turk, B. E., Chen, S., Chang, Y.-W., Wu, Z., Biemann, K., and Liu, J. O. (1997) Methionine aminopeptidase (type 2) is the common target for angiogenesis inihibitors AGM-1470 and ovalicin, *Chem. Biol. 4*, 461−471.
30. Eblen, S. T., Slack-Davis, J. K., Tarcsafalvi, A., Parsons, J. T., Weber, M. J., and Catling, A. D. (2004) Mitogen-activated protein kinase feedback phosphorylation regulates MEK1 complex formation and activation during cellular adhesion, *Mol. Cell. Biol. 24*, 2308−2317.
31. Mosmann, T. (1983) Rapid colorimetric assay for cellular growth and survival: application to proliferation and cytotoxicity assays, *J. Immunol. Methods 65*, 55−63.
32. Sambrook, J., Fritsch, E. F., and Maniatis, T. (1989) *Molecular Cloning: A Laboratory Manual*, 2nd ed., Cold Spring Harbor Laboratory Press, Cold Spring Harbor, NY.
33. Morrison, D. K., and Davis, R. J. (2003) Regulation of MAP kinase signaling modules by scaffold proteins in mammals, *Annu. Rev. Cell Dev. Biol. 19*, 91−118.
34. Johnson, G. L., and Lapadat, R. (2002) Mitogen-activated protein kinase pathways mediated by ERK, JNK, and p38 protein kinases, *Science 298*, 1911−1912.
35. Taunton, J. (1997) How to starve a tumor, *Chem. Biol. 4*, 493−496.
36. Zhang, Y., Griffith, E. C., Sage, J., Jacks, T., and Liu, J. O. (2000) Cell cycle inhibition by the anti-angiogenic agent TNP-470 is mediated by p53 and $p21^{WAF1/CIP1}$, *Proc. Natl. Acad. Sci.. U.S.A. 97*, 6427−6432.
37. Wang, J., Lou, P., and Henkin, J. (2000) Selective inhibition of endothelial cell proliferation by fumagillin is not due to differential expression of methionine aminopeptidases, *J. Cell. Biochem. 77*, 465−473.
38. Rodriguez-Nieto, S., Medina, M. A., and Quesada, A. R. (2001) A re-evaluation of fumagillin selectivity towards endothelial cells, *Anticancer Res. 21*, 3457−3460.
39. Yaffe, D., and Saxel, O. (1977) Serial passaging and differentiation of myogenic cells isolated from dystrophic mouse muscle, *Nature 270*, 725−727.
40. Yang, G., Kirkpatrick, R. B., Ho, T., Zhang, G.-F., Liang, P.-H., Johanson, K. O., Casper, D. J., Doyle, M. L., Marino, J. P., Jr., Thompson, S. K., Chen, W., Tew, D. G., and Meek, T. D. (2001) Steady-state kinetic characterization of substrates and metal-ion specificities of the full-length and N-terminally truncated recombinant human methionine aminopeptidase (type 2), *Biochemistry 40*, 10645−10654.
41. Datta, B., Datta, R., Ghosh, A., and Majumdar, A. (2004) Eukaryotic initiation factor 2-associated glycoprotein, p67, shows differential effects on the activity of certain kinases during serum-starved conditions, *Arch. Biochem. Biophys. 427*, 68−78.

BI049172P